Geotechnical and Geological Engineering (2006) 24: 523–549
DOI 10.1007/s10706-004-5832-6

The direct shear strength and dilatancy of sand–gravel mixtures

ALESSANDRO SIMONI[1,★] and GUY T. HOULSBY[2]
[1]*Dipartimento di Scienze della Terra e Geologico-Ambientali, Università di Bologna, Via Zamboni 67, 40126 Bologna, Italy*
[2]*Department of Engineering Science, Oxford University, Parks Road, Oxford OX1 3PJ, UK*

(Received 4 March 2004; revised 21 October 2004; accepted 3 November 2004)

Abstract. A total of 87 direct shear tests in a large direct shear-box apparatus have been used to investigate the strength and dilatancy of sand–gravel mixtures. This paper focuses on the differences in behaviour between a silica sand (yellow Leighton Buzzard sand) and sand–gravel mixtures obtained by adding fractions of two kinds of gravel to the sand. The purpose is to find a relation between the grain-size characteristics of the materials and the shearing resistance. Experimental results are analysed in terms of the frictional and dilatant contributions to the strength of mixtures as a function of their relative density, and are compared with dilatancy theories and empirical equations. The addition of gravel to the mixtures, even at low fractions (less than 0.1 by volume), causes an increase in peak friction angle (ϕ'_{peak}) which results both from higher dilatancy at failure (ψ_{max}) and higher constant volume friction angle (ϕ'_{cv}). Use of the minimum voids ratio (e_{min}) of the materials allows the data for the two families of mixtures to be normalized and interpreted in terms of ϕ'_{cv} and the ratio $(\phi'_{peak}-\phi'_{cv})/\psi_{max}$. The relationships between relative density (D_r), ψ_{max} and $\phi'_{peak}-\phi'_{cv}$ are only partly explained on a physical basis, so we develop empirical equations to predict the peak shear resistance of sand–gravel mixtures (up to gravel contents of 0.5) on the basis of easily measurable quantities. Such equations constitute a practical tool to overcome the problems arising from the impracticality of testing coarse material in the standard shear-box apparatus.

Key words. coarse granular material, direct shear test, empirical equations, minimum voids ratio, over-size particles, relative density.

1. Introduction

Laboratory testing of coarse granular material poses a problem because of the small dimensions of the standard shear-box apparatus. Although dependent on the testing device, the maximum grain size that can be tested rarely exceeds 10 mm with standard apparatus, and it is often necessary to limit the investigation to the sand fraction. Facing this problem, one can try to test a representative sample of material containing gravel using, for example, a fraction of the material passing a certain sieve (the scalping method), or a scaled material which maintains the shape of the grain size distribution (parallel gradation method). In either case, a method is needed to

★Corresponding author: Alessandro Simoni, Dipartimento di Scienze della Terra e Geologica-Ambientali, Universita di Bologna, via Zamboni 67, 40126 Bologona, Italy. e-mail: simoni@geomin.unibo.it

relate the shear strength of the whole material to that of the chosen sample. An alternative would of course be the acquisition of a suitably large shear test apparatus, but the costs will often not be justifiable by the importance of the work.

Such considerations apply to cohesionless materials, in which undisturbed sampling is (almost) impossible and which do not have special particle arrangements such as particular sedimentary structures. In this case, the behaviour of the material of a certain composition is primarily ruled by its density, which can be reproduced in laboratory reconstituted samples.

Assuming that, up to a certain fraction of coarse particles, the behaviour of the whole material is essentially ruled by the finer material, Fragaszy et al. (1990) developed an empirical procedure for determining the effects of introducing some floating "oversize particles" on the density of the soil "matrix" containing them. This method allows estimation of the average far-field matrix density which, according to Fragaszy et al., is primarily responsible for the behaviour of the whole mixture. The results of drained and undrained triaxial tests on the whole mixture and on the matrix only (compacted at the corresponding far-field matrix density) showed good agreement in terms of peak shear strength, for oversize particle fractions up to 0.5 by weight (Fragaszy et al., 1992). Differences were observed, however, in terms of volume or pore pressure changes. Samples of the matrix alone exhibited larger volumetric strains or higher pore pressures, as compared to whole mixture samples.

Similar efforts have been made to understand the behaviour of mixtures of various sizes. Attention has been directed towards the detection of a threshold fraction determining the influence of either component (Kumar and Muir Wood, 1999; Vallejo and Mawby, 2000), or on the accurate description of the behaviour of the mixture as a function of grading characteristics (Cola and Simonini, 2002) or "intergranular" and "interfines" void ratios (Thevanayagam and Mohan, 2000). In all the above cases, the presence of silt and/or clay particles in the mixture introduces additional variables, which make comparisons with sand–gravel mixtures difficult, if not impossible. When particle size falls below the sand/silt limit (0.074 mm), interparticle forces become important in determining the packing structure (Smalley and Dijkstra, 1991) and the particle shape tends to move away from sphericity and roundness (Rogers et al., 1994) which are more commonly found in coarser natural particles.

As far as the authors are aware, no other satisfactory results or systematic attempts to model the shear strength of sand–gravel mixtures, based on their relative proportions, have been published.

The effects of grain size and gradation on shear strength are of most interest here, since gradation is often obtained by adding coarser or finer fractions. Leslie (1969), using large drained triaxial tests, found that the peak shear strength of well-graded alluvial gravels slightly decreases (by 1° approximately) with maximum grain size, while the increase of the coefficient of uniformity ($C_u = D_{60}/D_{10}$) caused a significant increase in peak shear strength (40°–42.5° for C_u from 3 to 8

approximately). Kirkpatrick (1965) obtained similar effects due to the grain size (0.3–2 mm in his case) but was unable to draw any conclusions about the effects of grading.

The main objective of this work is to investigate the behaviour of coarse, poorly graded natural granular soils containing particles that are too big to be tested in a standard shear test apparatus. Based on the nomenclature proposed by Fragaszy et al. (1990), we take the boundary between matrix and oversize particles at 2 mm, and tested a poorly graded silica sand (matrix material) mixed with various fractions of two different kind of gravels (oversize particles). Given the importance of the direct link between peak shearing resistance and dilatancy of granular soils (Rowe, 1962), which can also be expressed in a practical and simplified form (Bolton, 1986), the concept of dilatancy is extensively used in the interpretation of the tests. The development of practical methods to relate the strength characteristics of the whole material to that of the matrix alone is also addressed.

We present the results of 87 shear box tests performed in a large apparatus at a constant normal stress (approximately 90 kPa) and widely varying relative densities. The possible influence of peculiar granular structures (e.g. anisotropy, metastable structures, etc.) and/or *in situ* stress conditions are not taken into account. The sample preparation technique was intended to minimize non-homogeneity within the granular structure.

Owing to its simplicity, and suitability for testing a wide range of geomaterials, the direct shear box is still widely used, especially in commercial work. Notwithstanding its limitations, primarily related to the non-uniformity of stresses and strains inside the sample, it has recently been demonstrated that a well designed apparatus can successfully minimize any undesirable effects, and provide reliable and meaningful results (Shibuya et al., 1997).

2. Shear Box Testing Device and Procedure

The shear box used was originally designed by Jewell (1980). It is 254 mm × 152 mm in plan, and the sample depth is approximately 150 mm. The bottom of the box and the upper plate are each rough, while the side walls are smooth (perspex or steel) and have been kept carefully polished during the tests. The shear load is applied to the lower part of the box, while the upper part is restrained against horizontal movement. The top platen, upon which the vertical load is applied, is fixed to the upper part of the box during testing, so that the two move entirely together. The vertical displacement is measured by two transducers placed on opposite corners of the upper half of the box, to detect any tendency for the box to tip (Figure 1). This configuration has the advantages that (a) the effects of wall friction on the transmission of vertical force to the shear surface are eliminated because soil grains do not move relative to the upper half walls, (b) the measured tilt of the upper half and top platen was always very limited, and so does not cause either a non-uniform distribution of vertical loads

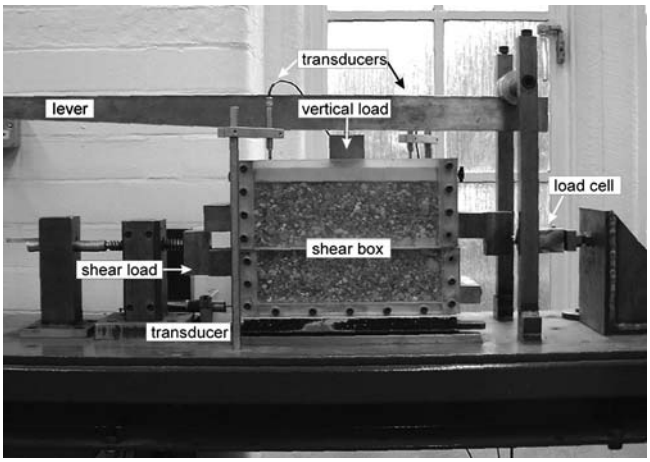

Figure 1. The direct shear box apparatus.

(which can favour progressive failure mechanisms) or undesirable variation of density.

The size of the opening between the upper and lower halves of the box constitutes another possible source of unwanted effects. A small aperture may restrict the development of the shear band, while a large opening causes stress reduction and material loss at the specimen edge. According to Shibuya et al. (1997), the space should be maintained at a constant value slightly larger than the thickness of a free shear band (approximately 10–20 times D_{50}). However, considerable practical difficulties arise when applying such a criterion to coarse material because the required size of opening would be several centimetres. Even using a membrane to prevent the collapse of the material at the edge, the effects of stress reduction during consolidation and shear would influence the results. A systematic investigation of the effects of opening size with respect to the grain size of the soil tested is outside the purpose of this work. We therefore fixed the initial opening between the two halves at 1 mm for all tests. During shear the spacing was free to vary, and in no case was there sufficient contraction to close this gap.

The samples were prepared and sheared in dry conditions. Given the wide range of grain sizes (0.1–20 mm), it was not possible to use a sample preparation technique such as dry pluviation, so the samples were prepared by rapidly pouring layers (approximately 20 mm thick) into the box, making sure, for each of the 7–8 layers, that segregation of particles did not occur. This technique provides samples of low density ($D_r = 0.1$–0.2) which where then vibrated to obtain the large range of densities that were tested. When the gravel fraction is 0.5 or higher, and the contacts between oversize particles increase, the vibration technique becomes less effective and mechanical compaction of each layer, prior to vibration, was required to achieve the densest packings. The state of compaction of the sample was monitored by measurements of sample height, until the required density was achieved.

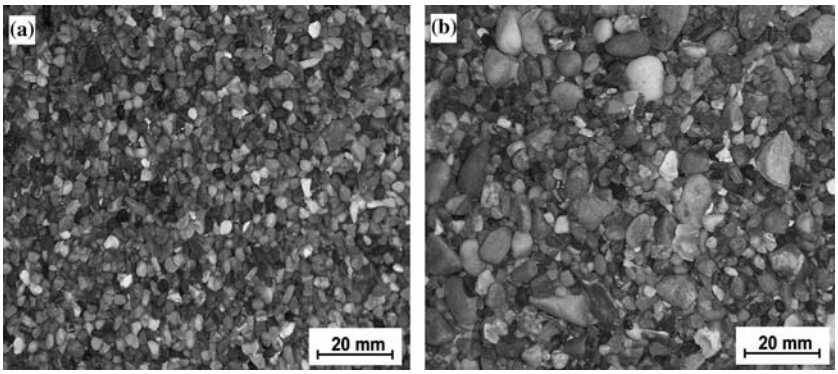

Figure 2. G06 (a) and G20 (b) gravels.

3. Materials

The materials used were obtained from Double Arches Quarry (Leighton Buzzard, UK) and consist of (a) a well graded, medium rounded to sub-angular silica sand, (b) a poorly graded, medium rounded to sub-angular gravel (Figure 2) and (c) a well graded, rounded to sub-angular gravel (Figure 2). The three materials are referred to as *sand*, *G06 gravel* and *G20 gravel* in the following. The main properties of the three materials are summarized in Table 1 and the grain size distributions are shown in Figure 3.

Mixtures of sand and gravel will be referred to by the initials of the gravel and the percentage of gravel by weight (for example: G0635 identifies a mixture containing 35% of gravel G06 and 65% of sand). Seven G06-mixtures and five G20-mixtures were tested with gravel fractions ranging from 0.1 to 0.6.

The limit states of compactness (e_{max} and e_{min}) of each mixture were measured on samples weighing approximately 5 kg. To obtain the maximum voids ratio, a measuring cylinder containing the sample was quickly turned upside-down to achieve a loose state. The minimum voids ratio was achieved by vibrating the mix at increasing stress levels (up to 90 kPa) without causing crushing. Various measurements on samples of the same material showed good repeatability, with voids ratio variations usually not exceeding 0.005. This corresponds to a maximum error for relative density determinations of approximately ± 0.01.

Table 1. Properties of soils

Soil	Maximum grain size (mm)	D_{60} (mm)	D_{10} (mm)	Coefficient of Uniformity, C_u	Specific gravity, G_s
Sand	2	0.81	0.21	3.87	2.65
Gravel G06	6	5.30	3.10	1.61	2.63
Gravel G20	20	9.10	3.90	2.33	2.63

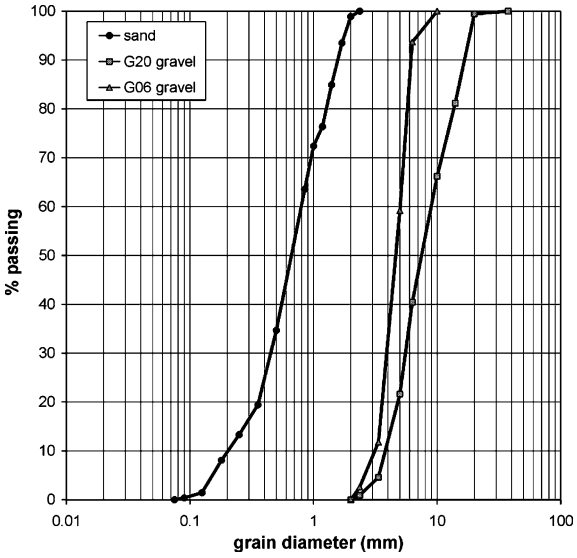

Figure 3. Grain size distribution curves for sand and gravels tested: mixtures were obtained by mixing different proportion of gravel and sand.

The definition of e_{max} and e_{min} as the voids ratios corresponding to the states of minimum and maximum compactness obtainable experimentally poses some problems in the choice of a uniquely valid technique for their measurement. However, a comparison between different techniques has demonstrated that the differences do not usually exceed 0.02 (Tavenas and La Rochelle, 1972).

The maximum and minimum voids ratios, as functions of the percentage by weight of the gravel fraction, are shown in Figure 4. Experimental points show an initial reduction of the voids ratios with increasing gravel fraction and reach a minimum corresponding to gravel fractions of 0.5 and 0.6 for G06 and G20 mixtures, respectively. A further increase of gravel fraction causes an increase in voids ratio up to the values obtained for the coarse material alone. The distance between the e_{min} and e_{max} curves for the same family of mixtures follows a similar trend, with this difference being a minimum for the densest mixtures.

In the case of G20 mixtures, the lowest e_{min} has been measured for G2060. Although it represents the highest gravel fraction tested, we expect it to be very close to the lowest e_{min}, given the overall trend.

Theoretical relationships can be used to express the voids ratio of binary mixtures, using ideal packing states of floating and non-floating oversized particles within a matrix (Fragaszy et al., 1990; Vallejo and Mawby, 2000). For brevity, we do not report the equations here. However, in the first case, floating oversized particles (gravel in our case) are assumed not to be in contact, and their inclusion does not affect the density of the matrix (sand). In the second case, non-floating gravel particles are in contact, and sand grains occupy the voids present in the

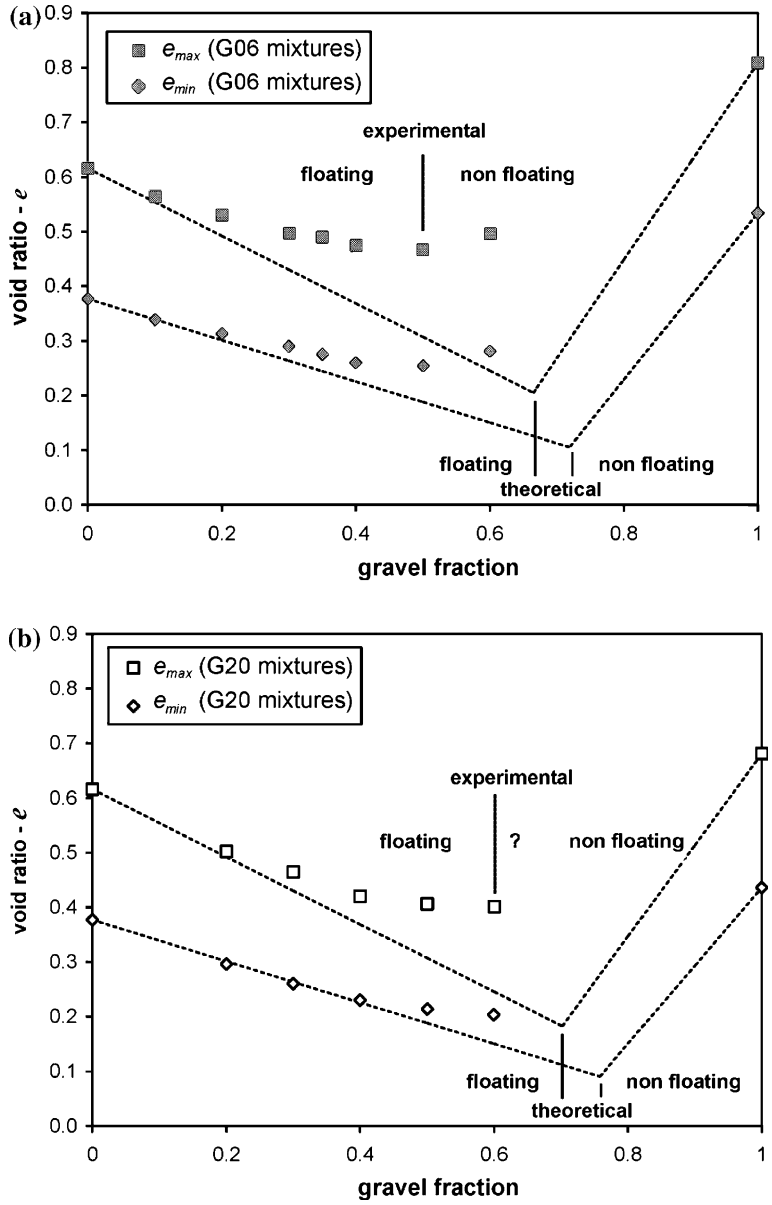

Figure 4. Limit states of compactness of G06 (a) and G20 (b) mixtures versus gravel fraction. Experimental points are compared to theoretical curves for floating and non-floating ideal states calculated using maximum and minimum void ratio for both components of the mixture: oversize particles and matrix soil.

gravel granular structure. The intersection of the two curves gives the theoretical minimum void ratio of the mixture, and coincides with the minimum fraction of oversize particles required to produce the ideal non-floating case. Such a state is

not unique, and depends on the density of both the oversized particles and the matrix soil. As can be seen in Figure 4, theoretical predictions, calculated using maximum and minimum densities for both oversize particles and matrix, tend to underestimate the voids ratio of the mixtures (either minimum or maximum) and to overestimate the fraction of coarse particles needed to achieve the maximum density which separates floating and non-floating states. The complexity of the actual grain-size distribution and its corresponding granular structure do not allow accurate density predictions by means of simple binary models. It is likely that two causes contribute to these discrepancies (a) the introduction of gravel particles, even when floating, influences the packing of the sandy matrix (i.e. surface effects and far-field density changes as reported by Fragaszy et al., 1990) and (b) gravel particles can be in contact within the granular structure well before the ideal non-floating state is reached.

It is not the purpose here to develop theoretical tools to describe the packing structure of heterogeneous aggregates. However, the simple density determinations performed have demonstrated that the gradation characteristics play an important role in the packing of the mixtures. In qualitative terms, (a) a well graded material (i.e. one with grain sizes extending over a rather large range) can achieve higher densities than a poorly graded one and (b) regular gradation (i.e. no gaps in the grading curve) favours higher densities for a given grain-size range. Fuller et al. (1907) and Rothfuchs (1935) showed that the highest densities could be obtained if the grain-size distribution of an aggregate follows the law:

$$p = 100\sqrt{\frac{a}{\mathrm{d}_{\max}}} \tag{1}$$

where p is the percentage passing the sieve of aperture a and $d_{\max}$ is the maximum grain size of the granular aggregate.

Figure 5 shows the theoretical curves obeying (1) compared to the grain-size distributions of the two families of mixtures. Distributions of mixtures G0650 and G2060, which gave minimum experimental voids ratio, approach most closely the theoretical curves.

The coefficient of uniformity ($C_{\mathrm{u}} = D_{60}/D_{10}$) shows a strong and consistent relationship with $e_{\min}$ and $e_{\max}$ for the mixtures (Figure 6), demonstrating again that the formation of dense packings of granular mixtures is strongly dependent on the grain-size distribution. Nevertheless, C_{u} alone cannot be used as a reliable grain-size descriptive tool. For example, it is the same for corresponding G06 and G20 mixtures up to a gravel fractions of 0.4, whilst the maximum density changes within this range.

In the following, it was found that the value of $e_{\min}$ is the most sensitive to grain-size distribution differences and, given its simplicity, was used in correlations with other variables. In particular, it appears to be a more useful parameter than the coefficient of uniformity in this context.

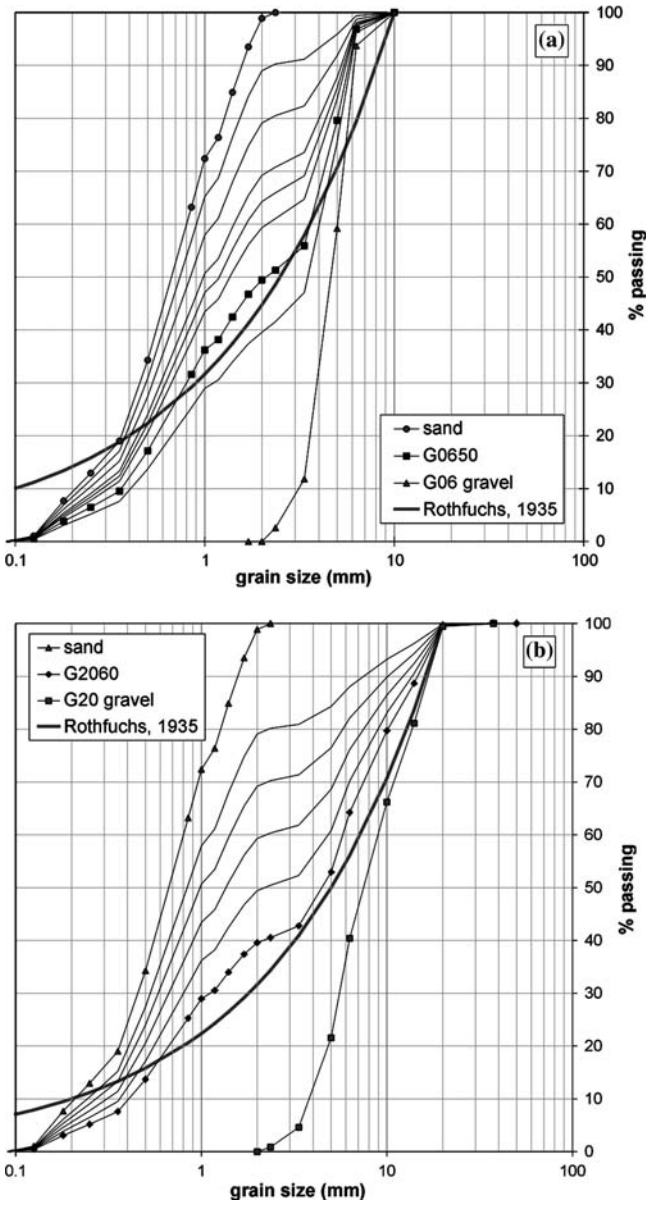

Figure 5. Grain-size distributions of all tested G06 (a) and G20 (b) mixtures. The highest density grain size distribution that follows the law proposed by Rothfuchs (1935) is shown for comparison.

4. Direct Shear Box Test Results

For each base material or mixture, a minimum of five direct shear box tests were performed at a range of relative densities (D_r) and at a constant normal pressure

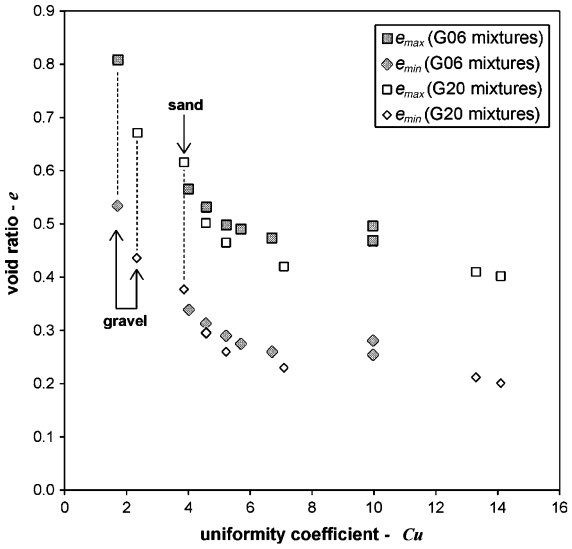

Figure 6. Limit states of compactness versus the coefficient of uniformity (C_u).

(90.8 kPa), giving a total of 87 tests. The main characteristics of the mixtures are summarized in Table 2, along with the D_r values used.

During each direct shear box test, the measured quantities were acquired every 5 s (corresponding to a shear displacement increment of about 0.028 mm), providing a detailed record of each experiment. The measured quantities were the shear load

Table 2. Properties of mixtures

Mixture	D_{60}(mm)	D_{60}(mm)	e_{max}	e_{min}	D_r values tested	ϕ'_{cv}(°)
Sand	0.81	0.21	0.62	0.38	0.95, 0.76, 0.54, 0.49, 0.40, 0.38, 0.31, 0.26, 0.22, 0.19	31.66
G0610	0.90	0.22	0.57	0.34	0.87, 0.72, 0.56, 0.36, 0.19	31.72
G0620	1.09	0.23	0.53	0.31	0.87, 0.70, 0.53, 0.41, 0.22	31.74
G0630	1.39	0.25	0.50	0.29	0.95, 0.76, 0.69, 0.60, 0.49, 0.37, 0.19	32.69
G0635	1.61	0.26	0.49	0.28	0.87, 0.78, 0.61, 0.45, 0.18	32.84
G0640	2.08	0.28	0.47	0.26	0.82, 0.57, 0.40, 0.33, 0.12	33.04
G0650	3.64	0.32	0.47	0.25	0.72, 0.58, 0.44, 0.30, 0.11	33.45
G0660	4.10	0.37	0.50	0.28	0.73, 0.54, 0.41, 0.33, 0.11	34.01
G06	5.03	3.16	0.81	0.53	0.90, 0.75, 0.59, 0.54, 0.45, 0.39, 0.34	30.99
G2020	1.11	0.24	0.50	0.30	0.83, 0.67, 0.56, 0.44, 0.24	33.05
G2030	1.42	0.26	0.47	0.26	0.83, 0.68, 0.47, 0.45, 0.35, 0.23	34.24
G2040	2.17	0.30	0.42	0.23	0.76, 0.65, 0.53, 0.39, 0.22	34.33
G2050	4.84	0.35	0.41	0.21	0.80, 0.75, 0.61, 0.49, 0.38, 0.25	35.27
G2060	5.81	0.40	0.40	0.20	0.73, 0.60, 0.47, 0.39, 0.22	35.86
G20	9.11	3.87	0.68	0.44	0.87, 0.78, 0.62, 0.64, 0.56	35.39

mobilized, the relative shear displacement in the horizontal direction, and the vertical displacement of the sample due to contraction or dilation of the soil. The vertical displacement was measured at opposite corners of the box, giving a measure of tilt which was, however, usually small. Some example results are shown in Figure 7, where the behaviour during shear of a medium dense sand ($D_r = 0.54$) is compared with a loose sample ($D_r = 0.22$) of the same material, and G0640 mixture of similar density ($D_r = 0.57$). It can be seen that the addition of gravel results in a substantial increase of the peak shear/normal stress ratio (τ/σ'_v), which can principally be attributed to an increase in the dilatancy contribution to the shear resistance of the mixture and partly also to an increase in the constant volume friction angle (ϕ'_{cv}). Such behaviour was regularly observed for tests on samples of sand–gravel mixtures: increasing either the density of the sample, or the fraction of coarse material, always gave an increase of peak shearing resistance.

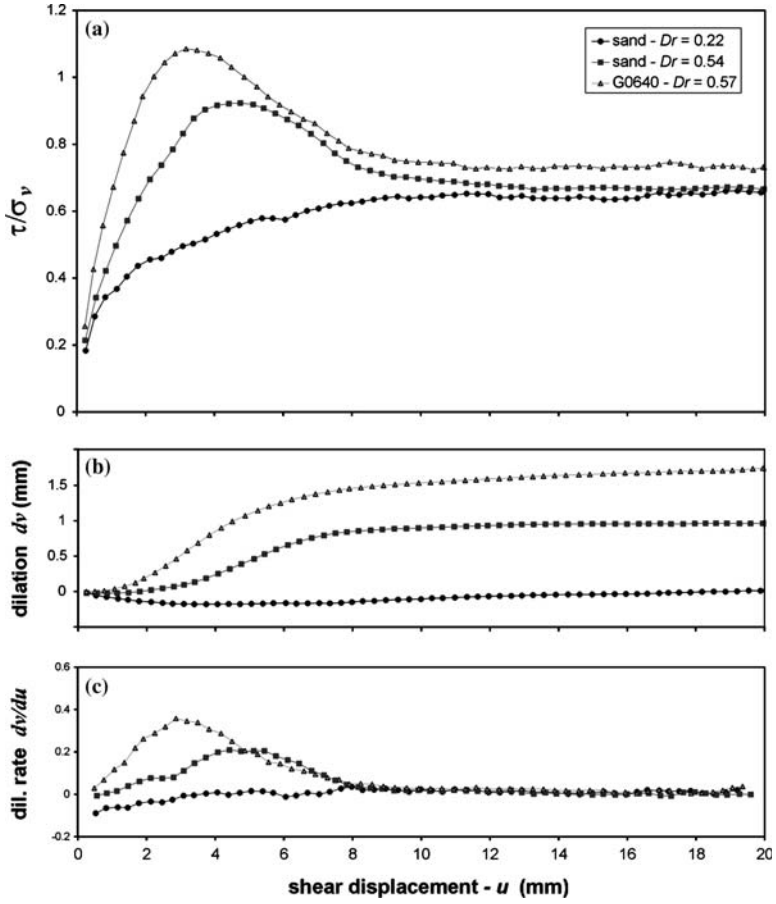

Figure 7. Example results of direct shear box tests. (a) shear stress ratio (τ/σ_v); (b) dilation (v) and (c) dilation rate (dv/du) versus shear displacement for tests on loose sand, medium dense sand and medium dense sand–gravel mixture.

The two measurements of vertical deformation (v) were averaged and related to the shear displacement (u) to calculate the rate of dilation ($\mathrm{d}v/\mathrm{d}u$). Assuming that the horizontal plane in the shear box is a zero extension line, the angle of dilation can then be deduced from the Mohr's circle of strain increments as:

$$\tan\psi = -\frac{\mathrm{d}\varepsilon_{yy}}{\mathrm{d}\gamma_{yx}} = \frac{\mathrm{d}v}{\mathrm{d}u} \tag{2}$$

where ε_{yy} and γ_{yx} are vertical compressive strain and shear strain. Because the displacements are measured over a very short interval of time, it was necessary to smooth the measured $\mathrm{d}v/\mathrm{d}u$ data to obtain useful results. It was found that a moving average of twelve successive readings ($\mathrm{d}u \approx 0.34$ mm) limited the scatter and gave a sufficiently smooth curve of dilation rate with shear displacement (Figure 7c). The maximum $\mathrm{d}v/\mathrm{d}u$ value was found to coincide, as expected, with the peak value of the shear/normal stress ratio, and was used to calculate the angle of dilation (ψ) at peak.

5. Analysis of Test Results

There are various methods which may be used to interpret a direct shear test. If it is assumed that the friction angle mobilized on the central plane is equal to the plane strain friction angle of the soil (ϕ'_{ps}), then the value $\tan^{-1}(\tau/\sigma'_v)$ gives an estimate of ϕ'_{ps}, but this is usually recognized as an underestimate. It is more appropriate to refer to the mobilized friction angle on this plane as direct shear friction angle:

$$\phi'_{\mathrm{ds}} = \tan^{-1}(\tau/\sigma'_v) \tag{3}$$

where τ and σ'_v are the shear and normal stresses.

If measurements of dilation and shear displacement are available, and assuming that the directions of the principal stresses are coincident with the directions of the principal plastic strain increments, it is possible to relate ϕ'_{ps} and ϕ'_{ds}, deriving the expression from the Mohr's circle of stress (Davis, 1968). This method of interpretation is often referred to as the coaxiality analysis. Such an analysis allows the amount by which the plain strain friction angle (ϕ'_{ps}) exceeds the direct shear angle of friction (ϕ'_{ds}) to be quantified by means of the following expression:

$$\tan\phi'_{\mathrm{ds}} = \frac{\sin\phi'_{\mathrm{ps}}\cos\psi}{1-\sin\phi'_{\mathrm{ps}}\sin\psi} \tag{4}$$

Alternatively, Rowe (1969) developed an elegant relation based on his flow rule (Rowe, 1962), which uses the plain strain constant volume friction angle ($\phi'_{\mathrm{cv,ps}}$) to relate ϕ'_{ps} and ϕ'_{ds}:

$$\tan\phi'_{\mathrm{ds}} = \tan\phi'_{\mathrm{ps}}\cos\phi'_{\mathrm{cv,ps}} \tag{5}$$

Both equations reduce to the following for zero dilation (constant volume):

$$\sin \phi'_{cv,ps} = \tan \phi'_{cv,ds} \tag{6}$$

Shear tests on granular materials can be successfully interpreted by using flow rules. These apply to plastically deforming soil, and relate the state of stress to incremental strains and the critical state shearing resistance of the soil. Theoretically derived flow rules have been proposed for instance by Taylor (1948) and Rowe (1962), and their predictions show good agreement with direct shear box test results on sands (Jewell, 1980; Pedley, 1990). In his comprehensive work, Bolton (1986, 1987) proposed a simple empirical fit to Rowe's flow rule and to experimental data gathered from 17 studies and performed on different kinds of sands worldwide:

$$\phi'_{ps} = \phi'_{cv,ps} + 0.8\psi \tag{7}$$

where ψ is the angle of dilation. Bolton also examined the relationship between friction angle, density and confining pressure. He developed empirical relationships, defining a relative dilatancy index, which in turn relates relative density (D_r) and confining pressure to the shear resistance and angle of dilation at peak. Given the utility of Bolton's equations and the difficulties associated with the correct theoretical interpretation of direct shear box test results, we have adopted Bolton's empirical framework for interpreting our experimental results. To accomplish this, we need a relationship between ϕ'_{ds} measured in the direct shear test and ϕ'_{ps} used in Bolton's empirical equations. Such a relationship can be obtained by combining Equations (4) and (7) or, alternatively, Equations (5) and (7), in each case eliminating ϕ'_{ps}. Figure 8(a) shows the results of combining Equations (4) and (7), expressed as a relationship between $\phi'_{peak,ds}-\phi'_{cv,ds}$ and ψ_{max}. The results can be expressed in a similar way to Equation (7):

$$\phi'_{peak,ds} - \phi'_{cv,ds} = b\psi_{max} \tag{8}$$

where the coefficient b is not a constant but is itself a function of ϕ'_{cv} and (to a much lesser extent) ψ, as shown in Figure 8(b).

Similar results are presented in Figures 9(a) and (b) by combining Equations (5) and (7). In both cases the coefficient b is close to the value of 0.8 used by Bolton, being in the range 0.71–0.75 for the relationship derived from the coaxiality analysis, and between 0.74 and 0.84 using Rowe's approach. In the two cases, the trend of variation of b with ϕ'_{cv} is, however, opposite. The deviations from linearity are sufficiently small that b can be taken as a constant for practical purposes.

The above observations indicate that the approach used by Bolton (1986) for plain strain conditions can be used also for the case of direct shear. A minor variation from the usual value of $b = 0.8$ is expected, depending on the ϕ'_{cv} value. Following these considerations, the experimental results are analysed in terms of direct shear friction angle (ϕ'_{ds}) and the experimental results are compared with a fit provided by empirical equations similar to Bolton's. In the following, all friction angles are direct shear friction angles ϕ'_{ds}.

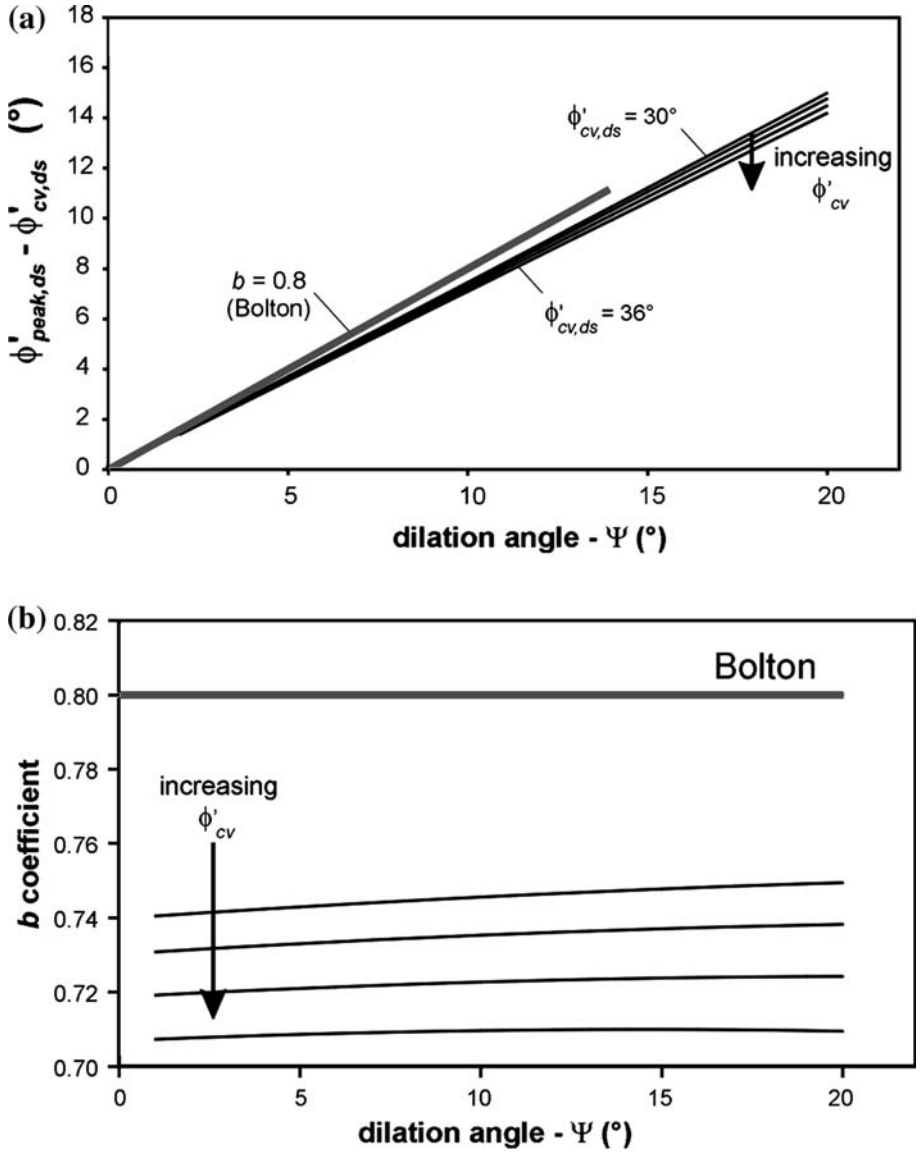

Figure 8. Adaptation of Bolton's empirical equation for direct shear condition using coaxiality assumption: (a) relationships are not perfectly linear as shown by slope variations with dilation angle; (b) effect of constant volume friction angle and dilation on *b* coefficient.

5.1. CRITICAL STATE FRICTION ANGLE

The critical state friction angle represents the minimum shear strength that a soil can display. It is mobilized when a sample shears at constant volume. Besides being a very useful design parameter, it is fundamental to the interpretation of shear test

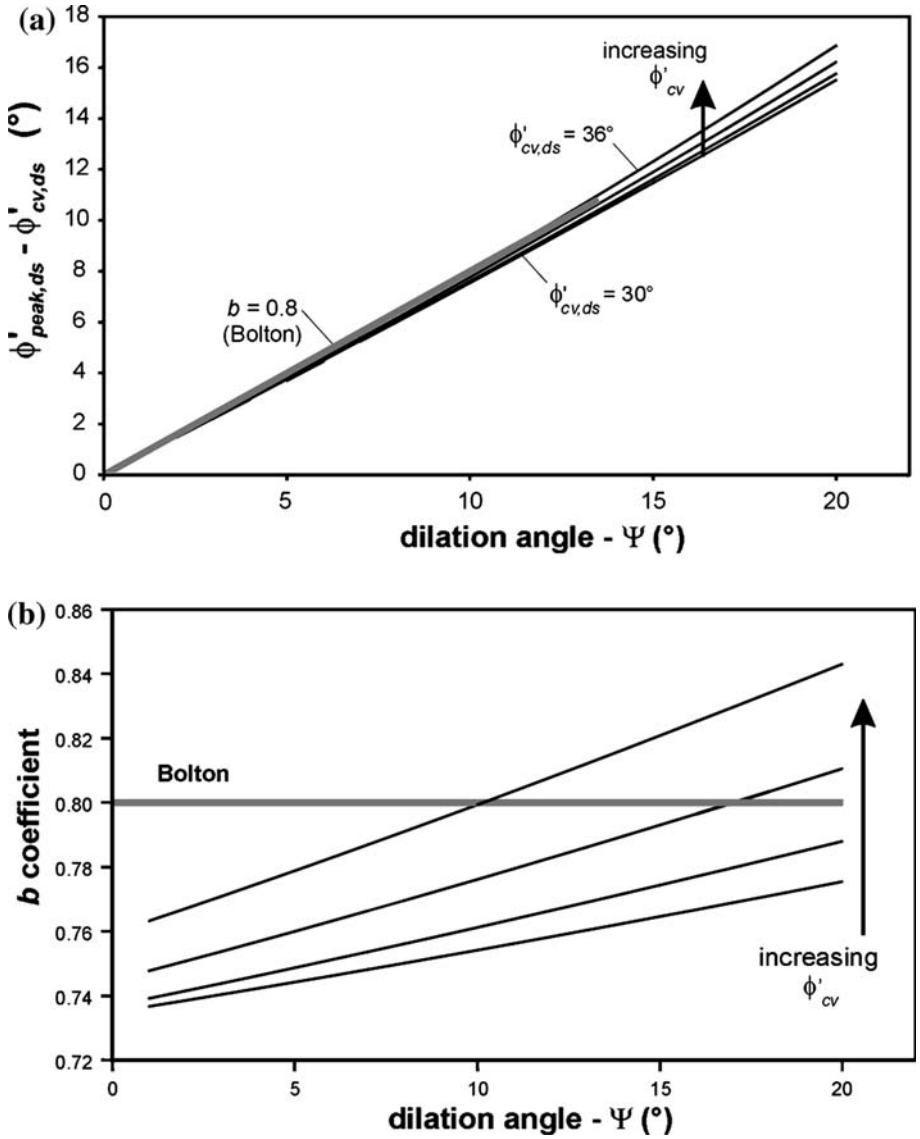

Figure 9. Adaptation of Bolton's empirical equation for direct shear condition using Rowe's assumption: (a) relationships are not perfectly linear as shown by slope variations with dilation angle; (b) effect of constant volume friction angle and dilation on *b* coefficient.

data in the light of dilatancy theories. Several methods can be used to obtain the critical state shearing resistance from the results of direct shear test data. They rely on the interpretation either of single tests or multiple tests taken together. Examples are of these analyses now described.

The direct measurement of the mobilized friction angle at large strains and zero dilation rate (method a) is a straightforward option.

Alternatively Taylor's (1948) energy correction ($\tau/\sigma'_v + \mathrm{d}v/\mathrm{d}u$) can be plotted against shear displacement (u). In this case, according to Taylor's theory, $\tau/\sigma'_v + \mathrm{d}v/\mathrm{d}u$ should take a constant value $m = \tan\phi'_{cv}$ (method b).

When multiple test results are available, by plotting $(\tau/\sigma'_v)_{peak}$ against $(\mathrm{d}v/\mathrm{d}u)_{peak}$ the data would be expected to fall on a line with an intercept equal to $\tan\phi'_{cv}$ at $(\mathrm{d}v/\mathrm{d}u)_{peak} = 0$, (method c).

Again using multiple tests, by plotting ϕ'_{peak} against ψ (measured at peak strength) a best fit line is obtained giving ϕ'_{cv} as the shearing resistance of a sample which would exhibit zero dilatancy at failure (method d). Method d requires at least two shear tests at different densities.

Methods based on the results of multiple tests are more reliable since they minimize the influence of errors in any one test. Similarly, measurements taken at small strains (peak conditions) are expected to be more reliable than at large strains (as required for method a), when heterogeneities in stress and strain are more likely to develop.

We adopted method d because of the above considerations, and because it facilitates the following comparison with Bolton's empirical equations. For each material, ϕ'_{cv} was determined from a series of at least five tests at a range of densities. The tests showed a good correlation, as for the example in Figure 10, where a comparison with other methods is also reported. All the linear regression lines, fitting the experimental data for any one material, have an R^2 value higher than 0.97. The ϕ'_{cv} value for sand is 31.66°, while the two gravels showed substantially different values. Given that the mineralogy and the particle shapes of the G06 and G20 gravels are

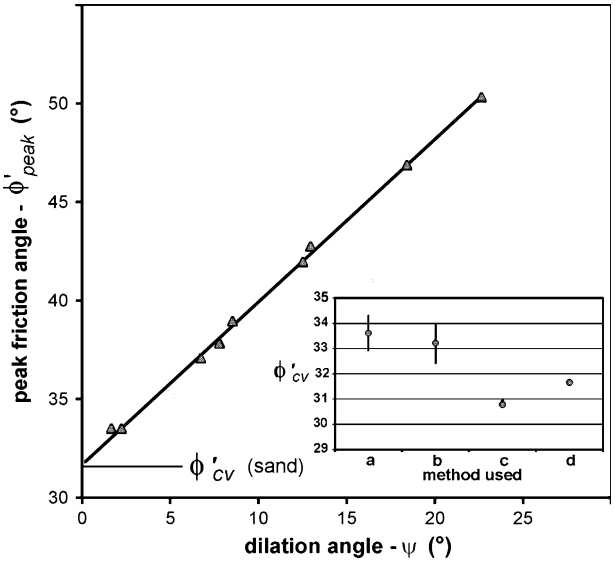

Figure 10. Method used for the determination of the critical state friction angle (method d); the example reported refers to sand. The small chart compares the results obtained using alternative methods (a–c as reported in the text) to estimate the critical state shearing resistance from DSB tests.

similar, the observed differences are primarily attributable to differences in grain-size (Figure 3). The relatively single sized G06 ($C_u = 1.59$) has a ϕ'_{cv} of 30.99° and the more heterogeneous G20 ($C_u = 2.35$) has a $\phi'_{cv} = 35.39°$. The range for sand–gravel mixtures varies from 31.72° to 35.86°. Plotting the measured ϕ'_{cv} versus the gravel fraction by weight (Figure 11a), distinct relations emerge for the two families of

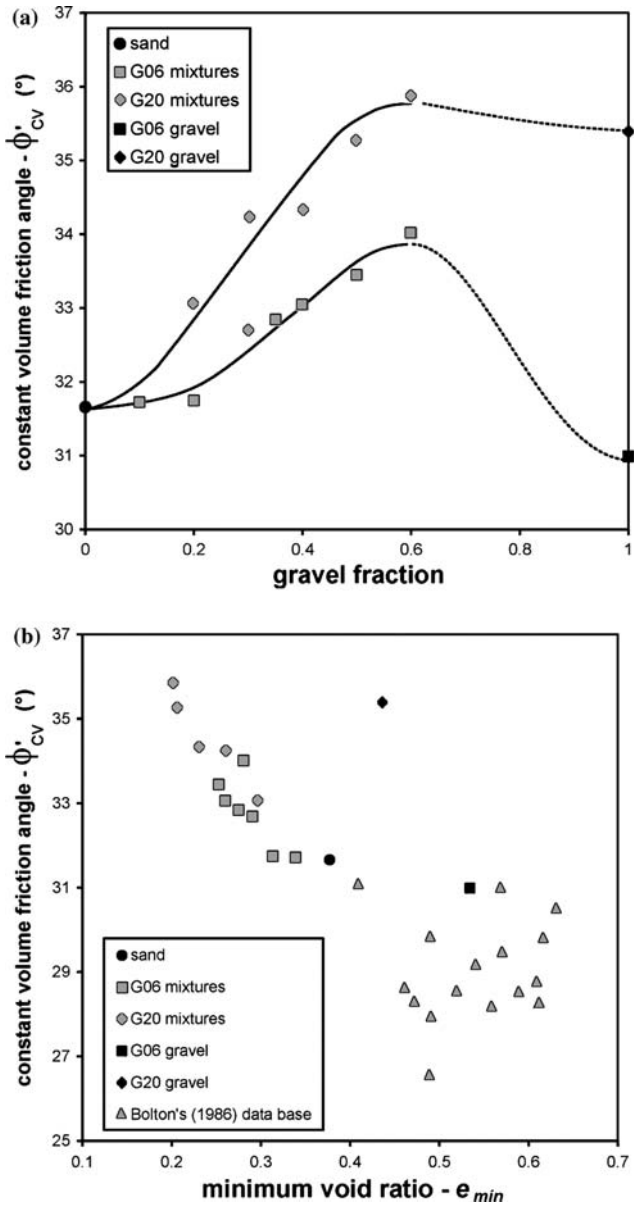

Figure 11. Results of critical state friction angle determination versus gravel fraction (a) and minimum void ratio (b) in comparison with results reported in Bolton (1986).

mixtures. Clearly the grain-size distribution has an important influence on the behaviour. Given the difficulties connected with the definition of a simple and objective index describing grading characteristics, the observed ϕ'_{cv} was related to indirect but objective measures such as the minimum and maximum densities. It was found that, with some scatter, ϕ'_{cv} could be related to e_{min}. Thus in Figure 11b, the experimental points for the mixtures are approximately grouped along a single line, for both G06 and G20 mixtures. Experimental data taken from Bolton (1986) for sands have been included in the chart. To make the comparison possible, the triaxial compression and plane strain critical state friction angles (which Bolton assumes to be equal) are related to the direct shear value by Equation (6).

Although there is scatter due to the variety of materials, in terms of mineralogy and particle shape, Bolton's data, mostly referring to poorly graded (high e_{min}) sands, generally confirm the trend observed for the gravel/sand mixtures.

Important observations can be made about the derived values of ϕ'_{cv}: (a) an increase in gravel fraction causes an increase in the critical state friction angle of sand-gravel mixtures (for the fractions with floating oversize particles), (b) the critical state friction angle is related to the grain-size distribution, materials with the ability to maximize their packing density (low e_{min}) showing relatively higher values of resistance, (c) e_{min} can be taken as an indirect index of grain-size characteristics and relates well to the critical state friction angle for granular materials which have similar mineralogy and grain shape.

5.2. PEAK FRICTION ANGLE AND DILATANCY

In this work, the effect of different confining pressures has not been considered: the vertical stress was kept constant in all tests at a relatively low value (90.8 kPa) to eliminate any effects of particle crushing. Crushing effects occur at higher pressures in a silica sand, rich in quartz grains (Feda, 2002) such as Leighton Buzzard sand. Bolton (1987) observed that the tendency for particles to crush under shear is not appreciable when the mean stress is lower than about 150 kPa, allowing dilation to be treated as a function only of density below this stress. This implies that the variables for examination reduce to $\phi'_{peak}-\phi'_{cv}$, ψ_{max} and D_r. Empirical equations like those proposed by Bolton are used to describe the relationships between these variables in the direct shear test. Bolton's equations for low stress level reduce to:

$$\phi'_{peak} - \phi'_{cv} = 0.8\psi_{max} = 5I_R \tag{9}$$

where $I_R = 5D_r - 1$, but subject to $I_R \geq 0$.

The tests on sand–gravel mixtures cannot be fitted well by Equation (9). Figure 12 shows schematically the original equations and the observed trends for the sand gravel mixtures. The upper diagrams show the general trends, and the lower ones the data from the G06 mixtures. The same trends were observed for G20 mixtures.

The results of tests on each mixture, in terms of $\phi'_{peak} - \phi'_{cv}$ and ψ_{max} are generally consistent. By fitting the points with linear regression lines passing through the

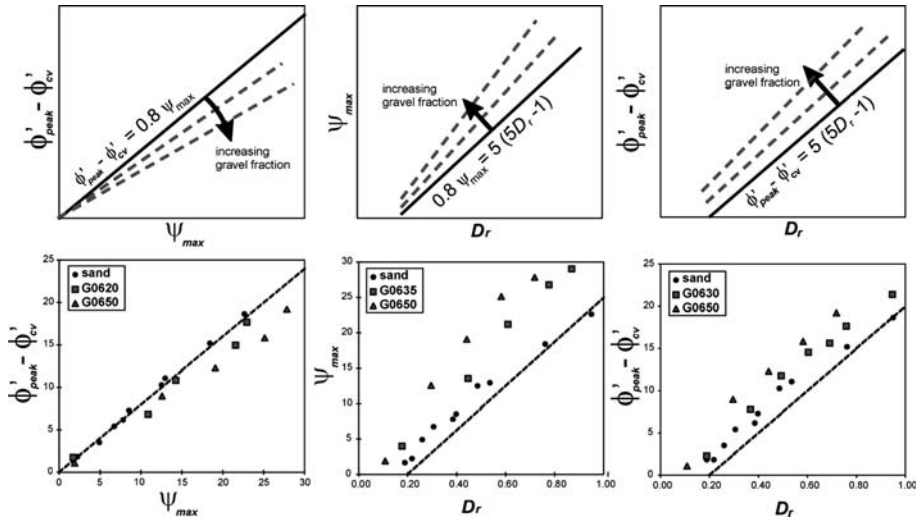

Figure 12. Application of Bolton's empirical equations, to sand–gravel mixtures. Upper charts: schematic representation of variation from Bolton's expressions. Lower charts: results of tests conducted on sand and G06 mixtures.

origin and described by Equation (8), a progressive decrease in the value of b with an increase of gravel fraction was observed. Such a trend cannot be fully explained either by Bolton's original equation, nor by modifying it to direct shear conditions through the coaxiality analysis (4) or Rowe's flow rule (5), both of which resulted in a slight dependence of b on $\phi'_{cv.}$ Figure 13 shows the comparison and highlights the significant drop in the proportion (b) of contribution from dilation to peak shear

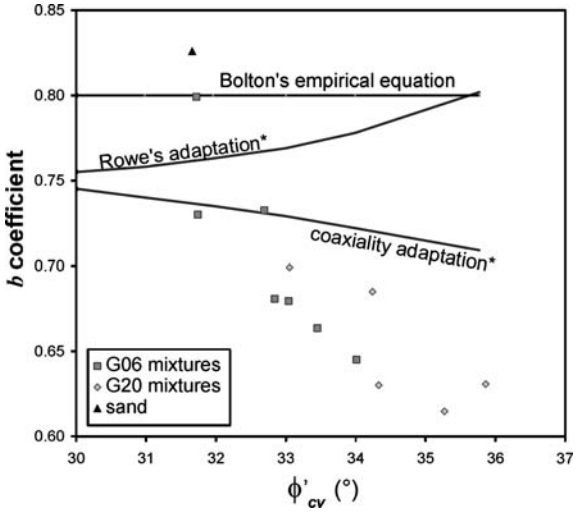

Figure 13. Comparison between experimentally determined variation of $(\phi'_{peak}-\phi'_{cv})/\psi_{max}$ ratio (b coefficient) with the constant value proposed by Bolton (1986) and adaptations derived theoretically.

resistance observed for gravel/sand mixtures. In summary, an increase of gravel fraction increases ϕ'_{cv} and ϕ'_{peak} but causes a decrease in the $(\phi'_{peak} - \phi'_{cv})/\psi_{max}$ ratio (b coefficient), up to gravel fractions of about 0.5.

Note that (as for ϕ'_{cv}, Figure 11) the b coefficients for the two different families of mixtures (G06 and G20) fall on two different curves if plotted against gravel fraction directly (Figure 14), whilst they align almost along a single line if plotted against e_{min} (Figure 15). The grading characteristics of the material, indirectly measured by e_{min}, seems to be a possible key for interpreting the results, although in this case it is difficult to hypothesize a physical basis for such behaviour.

It has been shown that the addition of gravel to sand results in a complex set of changes in the shearing resistance of the mixture. These changes are significant even at low gravel fractions (0.1–0.2 by weight) and reach a maximum at a gravel fraction of 0.5–0.6, which corresponds to minima in the curves for e_{min} and e_{max} for the two families of mixtures (Figure 5) and coincides with the transition from floating and non-floating states. The changes consist of an increase in constant volume friction angle (ϕ'_{cv}) and maximum angle of dilation (ψ_{max}) at comparable relative density (Figures 11 and 12). The relationship between the maximum measured angle of dilation (ψ_{max}) and the dilatancy contribution to peak shear resistance ($\phi'_{peak}-\phi'_{cv}$) changes as well, showing a progressive decrease in b value (Figures 12 and 14).

In spite of the fact that the sand-gravel mixtures show a decreasing $(\phi'_{peak}-\phi'_{cv})/\psi_{max}$ ratio, the overall peak resistance increases with gravel content, for a similar D_r. This is due to the increase in ϕ'_{cv} (Figure 11) and to the increase in ψ_{max} (Figure 12). In

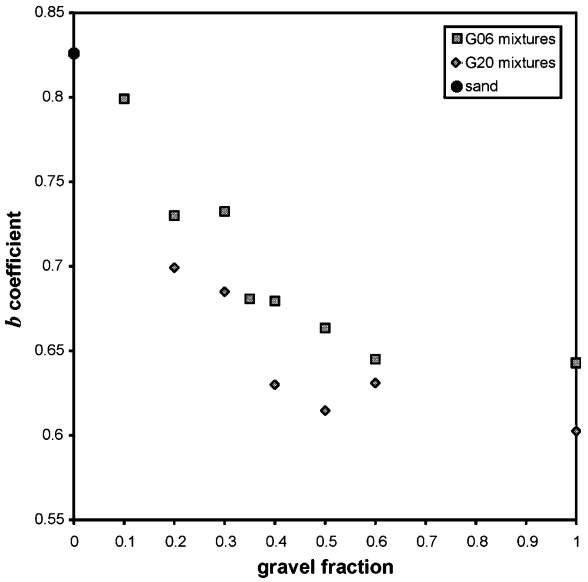

Figure 14. Variation of b coefficient with gravel fraction.

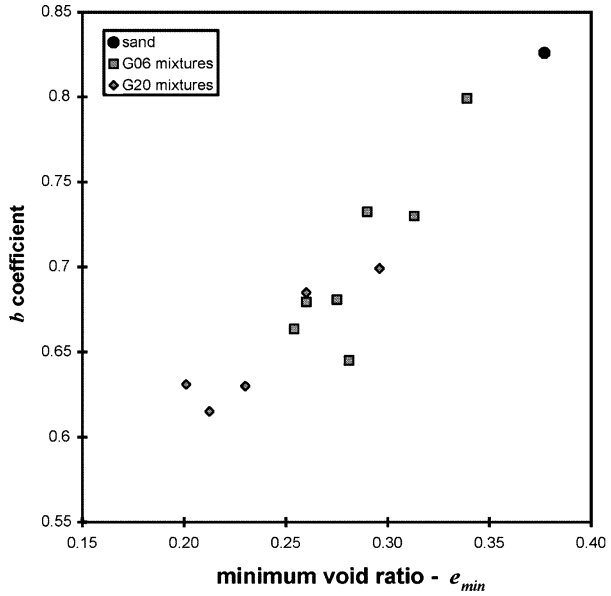

Figure 15. Variation of b coefficient with minimum void ratio.

Figure 16, ϕ'_{peak} is related to D_r for the two different families of mixtures. The three lines on each plot give (from bottom to top) the approximate correlation for the sand, and for gravel fractions of 0.3 and 0.5. The overall trend in ϕ'_{peak} results from a combination of changes in ϕ'_{cv}, ψ_{max} and $(\phi'_{peak}-\phi'_{cv})/\psi_{max}$ ratio.

5.3. EMPIRICAL EQUATIONS

We seek now simple empirical equations to describe the strength characteristics of the sand when mixed with either of the gravels tested. Such equations may be applicable to other similar materials. Since shear tests on coarse granular materials are often difficult, we seek expressions which could be useful for practical purposes, *i.e.* relations based on easily measurable parameters.

The measured ϕ'_{cv} values show a strong relationship with e_{min} (Figure 11b). By considering the difference between the minimum void ratio of the sand-gravel mixtures and the minimum void ratio of the sand alone ($e_{min,\ sand} - e_{min,\ mixture}$), it is possible to obtain a relationship describing the variation of ϕ'_{cv}:

$$\phi'_{cv,mixture} - \phi'_{cv,sand} = 18 \cdot \left(e_{min,sand} - e_{min,mixture}\right) \tag{10}$$

Figure 17 shows Equation 10 and the experimental points to which it was fitted, keeping ϕ'_{cv} of the sand as a fixed intercept. A more complex non-linear expression would clearly provide a better fit, but is hardly justified by the data. Once again, however, use of the minimum void ratio allows the data from two different families of mixtures (G06 and G20) to be combined. The decrease of $e_{min,mixture}$ with

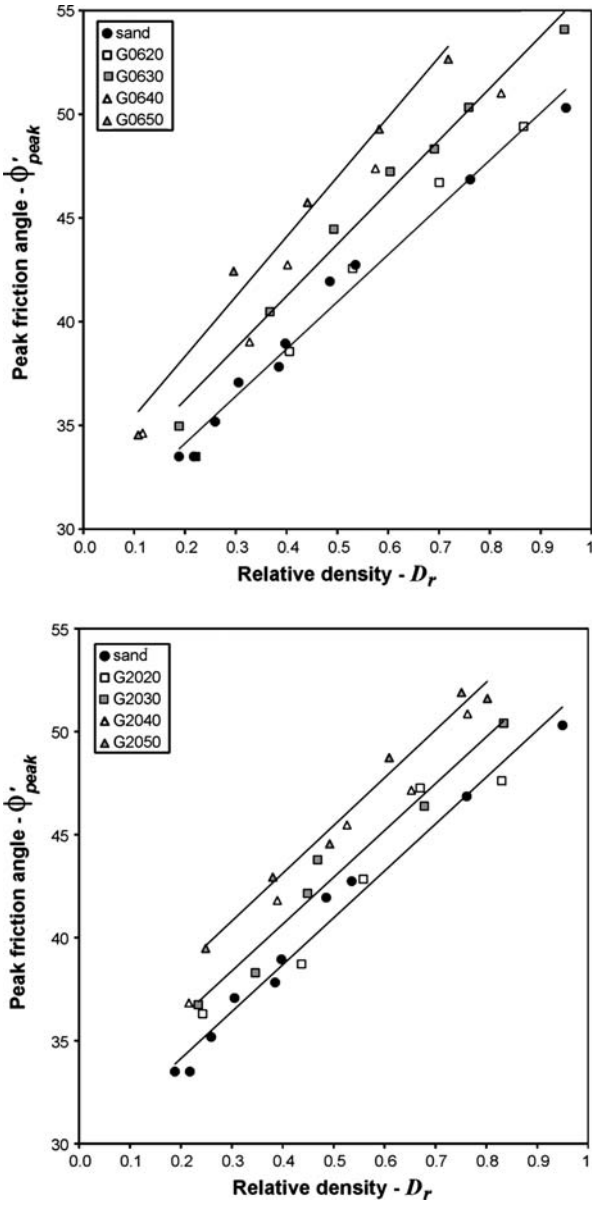

Figure 16. Peak friction angle versus relative density for sand, G06 mixtures and G20 mixtures. Not all the results are displayed, the fitting lines are for the sand and mixtures containing gravel fractions of 0.3 and 0.5 by weight.

increasing coarse material in the mixture is related to the increasing variety of particle sizes in the mixtures (see Figures 4, 5 and 6), which favours a denser packing with smaller particles filling voids between coarser particles.

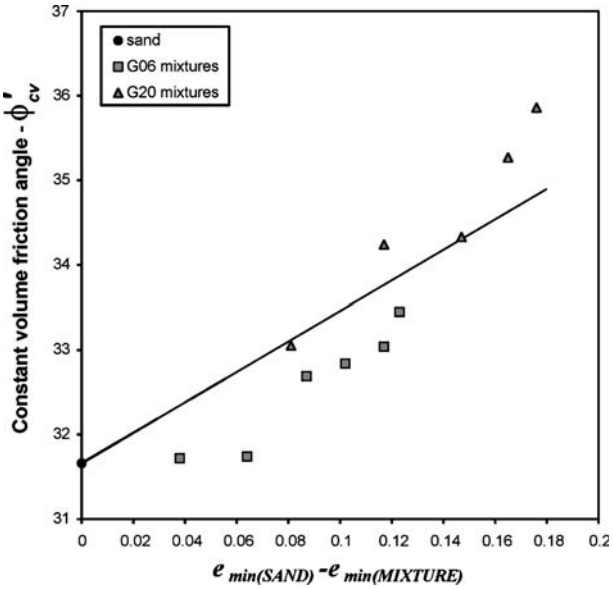

Figure 17. Empirical equation describing the variation of critical state friction angle of mixtures with e_{min} The line fits data for mixtures up to gravel fractions of 0.5 and has a fixed intercept corresponding to the constant volume friction angle of the sand.

To describe the complex interactions ruling the dilatancy contribution to the peak friction angle ($\phi'_{peak}-\phi'_{cv}$), involving peak angle of dilatancy and relative density, we take Bolton's equations as the starting point and modify them as required. Equation (9) effectively relates three interdependent variables (D_r, ψ_{max} and $\phi'_{peak}-\phi'_{cv}$). There are different possible ways to fit experimental data to this type of equation, and once two of the three relationships have been established the third one follows. The procedure adopted here is the simplest possible. Linear regression has been applied to the data pertaining to any particular mixture (5–7 direct shear box tests at different densities) in each of the three planes: ($\phi'_{peak}-\phi'_{cv}$, ψ_{max}), (D_r, ψ_{max}) and (D_r, $\phi'_{peak}-\phi'_{cv}$). The coefficients obtained (slopes and/or intercepts) for each mixture, up to a gravel fraction of 0.5, have been plotted against $e_{min,sand} - e_{min,mixture}$ and then regression analysis used to find an appropriate expression for the variations. This procedure follows the earlier observation that e_{min} provides a useful index of the grading characteristics of the material.

Bolton's Equation (7) was modified by substituting for the constant 0.8 an expression describing the variation of the b coefficient (8):

$$(\phi'_{peak} - \phi'_{cv})_{mixture} = (0.8 - 1.1(e_{min,sand} - e_{min,mixture})) \cdot \psi_{max} \tag{11}$$

Figure 18 shows the trend of the b coefficient. The fitting line has an intercept of 0.8, hence Equation (11) reduces to Bolton's original equation when no gravel is present.

The relative density has to be related simultaneously to $\phi'_{peak}-\phi'_{cv}$, and ψ_{max}. To obtain such relationships, it is possible to fit the experimental points in the plane

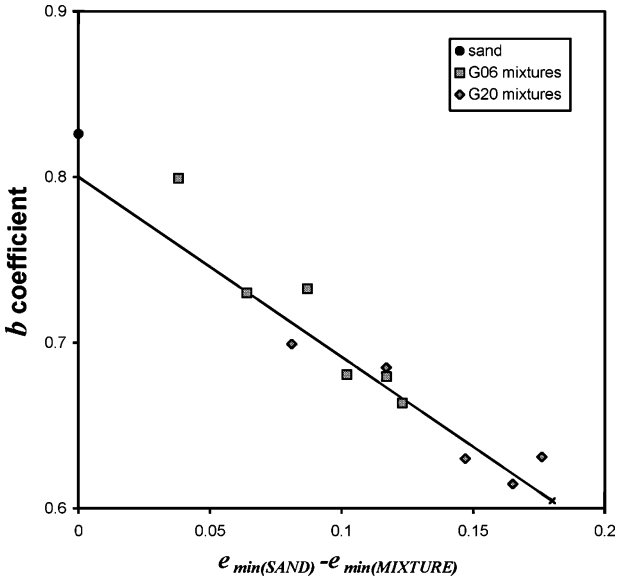

Figure 18. Empirical equation describing the variation of b coefficient. Experimental points are for mixtures up to 0.5 gravel fraction.

($\phi'_{peak}-\phi'_{cv}$, I_R) or alternatively in the plane (ψ_{max}, I_R). The results are very similar and are most easily expressed by adopting a modified definition of I_R:

$$I_{R,mixture} = 5D_{r,mixture} - (1 - 4.3 \cdot (e_{min,sand} - e_{min,mixture})) \tag{12}$$

whilst retaining Bolton's original equation:

$$(\phi'_{peak} - \phi'_{cv})_{mixture} = 5I_{R,mixture} \tag{13}$$

This completes the relationships between the three variables, since the same term appears on the left hand side of Equations (11) and (13).

The empirical equations must be considered valid only at low normal pressures (<150 kPa) when particle crushing does not occur. They allow prediction of the peak friction angle of a sand-gravel mixture in which the gravel fraction is low enough to exist in a non-floating state; i.e. below the fraction giving the lowest $e_{min,mixture}$. To make such a prediction, experimental requirements are simple and can be performed with common apparatus. They include shear testing only the sand fraction (to obtain $\phi'_{cv,sand}$) and measuring the minimum density of the matrix alone (sand) and of the sand-gravel mixture to give ($e_{min,sand}-e_{min,mixture}$). The choice of the sand matrix as reference material derives from the satisfactory fit of experimental data and from its suitability to practical purposes (no oversize particles need to be tested).

Figure 19 compares the predictions of Equations (10), (12) and (13), in terms of ϕ'_{peak} with experimentally measured values. The points show an even distribution around the 1:1 line and no significant trend can be detected for the residual error.

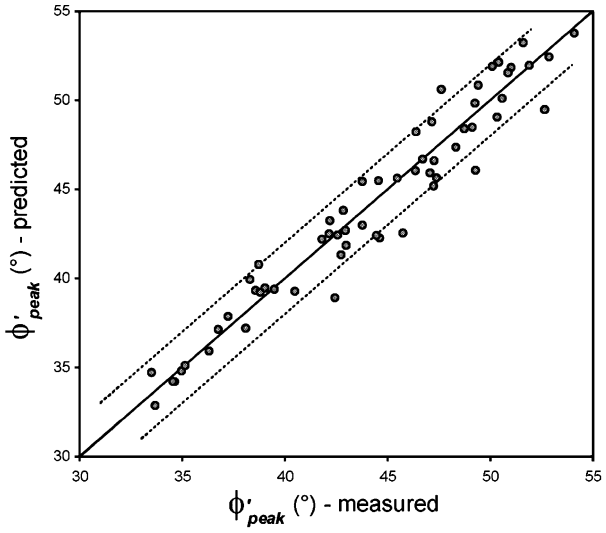

Figure 19. Comparison between measured peak friction angle and predictions obtained using the proposed empirical equations. The dashed lines represent $\pm 2°$ from the line of equality.

For all but a handful of mixtures the angle of friction is predicted within 2°, whilst the values measured cover a range of about 20°. The figure indicates that the empirical equations can approximate the behaviour of the sand-gravel mixtures tested for the entire range of densities. The precision is generally satisfactory, although this judgement clearly depends on specific applications.

If, alternatively, the predicted ϕ'_{peak} is calculated by means of Equation (10) and (11), a better fit to the strength can be achieved, but this procedure is not practical, since the maximum dilation at failure ($\psi_{\max}$) requires an experimental measurement.

Summary and Conclusions

Heterogeneous, non-cohesive granular materials, including gravel-size particles, are quite common. They are widely represented among onshore alluvial deposits, where their exploitation is of commercial importance. Furthermore, the use of natural or artificial fills containing coarse particles is increasingly common. The description of the behaviour of such materials, including their strength and deformation characteristics, is necessary for practical applications such as quarrying and road construction. Shear strength determination can become a problem when laboratory tests cannot be performed due to particle size limitations when conducting standard shear tests.

The results of a series of large direct shear box tests on two families of sand–gravel mixtures have been presented, focusing on the differences in strength and dilatancy caused by the introduction of increasing gravel fractions. Two different medium-rounded to subangular gravels have been added in different proportions to Leighton

Buzzard sand, and the mixtures obtained were tested to investigate their strength and dilatancy characteristics. Shear tests were conducted at a low confining pressure on a wide range of relative densities, to eliminate the effect of confining pressure and grain crushing on the behaviour of the materials. The results clearly indicate that even at low gravel fractions (0.1–0.2), when the oversize particles are in a floating state within the sand matrix, the peak strength, constant volume strength and maximum dilatancy rate of the mixtures, are all higher than those for the sand at the same density. For both families of mixtures tested, trends in the variation of three related variable (ϕ'_{peak}, ϕ'_{cv}, and ψ_{max}) are quite consistent up to gravel fractions of approximately 0.5, when contacts between the large particles become more important and there is a transition to a non-floating state (in which the voids between gravel particles in contact are filled by the sand matrix).

The addition of coarse particles to a sand causes several effects to the structure of the resulting material. Neglecting particle mineralogy and shape, which did not vary significantly in this study, the addition of coarse particles resulted in a decrease of the limit states of compactness (e_{min}, e_{max}) up to a gravel fraction of 0.5 and 0.6, respectively for the two families of mixtures. The e_{min} and e_{max} parameters are easy to measure and serve as indices of the grading characteristics. This proves useful in describing the experimental results, and e_{min} can be satisfactorily related to the strength and dilatancy characteristics of the mixtures. The variations in the frictional and dilatant contributions to strength induced by the addition of oversize particles can be successfully interpreted at low confining pressures in terms of relative density (D_r) and reduction in minimum void ratio due to gravel addition ($e_{min,sand} - e_{min,mixture}$). We adapted Bolton's empirical equations to describe the behaviour of poorly sorted granular material (sand-gravel mixtures), and propose a simple method to derive and ϕ'_{peak} and ϕ'_{cv}, based on the physical and shear strength properties of the sand (e_{min}, and ϕ'_{cv}) and the physical properties of the mixture (e_{min} and D_r). Such empirical equations are strictly valid only for materials and conditions similar to those of our experiments. They are applicable only when no grain crushing occurs, hence at low confining pressures and depending on grain mineralogy. Further experiments would be required for the investigation of the role of mineralogy, grain shape and confining pressure.

References

Bolton, M. D. (1986) The strength and dilatancy of sands. *Géotechnique*, **36**(1), 65–78.

Bolton, M. D. (1987) The strength and dilatancy of sands. Discussion. *Géotechnique*, **37**(1), 219–226.

Cola, S. and Simonini, P. (2002) Mechanical behaviour of silty soils of the Venice lagoon as a function of their grading characteristics. *Canadian Geotechnical Journal*, **39**, 879–893.

Davis, E. H. (1968) Theories of plasticity and failures of soil masses. In *Soil Mechanics, Selected Topics* (editeb by I.K. Lee), Butterworth, London.

Feda, J. (2002) Notes on the effect of grain crushing on the granular soil behaviour. *Engineering Geology*, **63**, 93–98.

Fragaszy, R. J., Su, W. and Siddiqi, F. H. (1990) Effects of oversize particles on the density of clean granular soils. *ASTM, Geotechnical Testing Journal*, **13**(2), 106–114.

Fragaszy, R. J., Su, J., Siddiqi, F. H. and Ho, C. L. (1992) Modeling strength of sandy gravel. *ASCE, Journal of Geotechnical Engineering*, **118**(6), 920–936.

Jewell, R. A. (1980) Some effects of reinforcement on the mechanical behaviour of soils. PhD Thesis, Cambridge University.

Kirkpatrick, W. M. (1965) Effects of grain size and grading on the shearing behaviour of granular materials, *Proceedings of the 6th International Conference on Soil Mechanics and Foundation Engineering*, Vol. 1, 273–277.

Kumar, G. V. and Muir Wood, D. (1999) Fall cone and compression tests on clay-gravel mixtures. *Geotechnique*, **49**(6), 727–739.

Leslie, D. D. (1969) Relationship between shear strength, gradation and index properties. *Proceedings of the 7th International Conference on Soil Mechanics and Foundation Engineering*. Speciality Session No. 1, 212–222.

Pedley, M. J. (1990) The performance of soil reinforcement in bending and shear. PhD Thesis, University of Oxford.

Rogers, C. D. F., Dijkstra, T. A. and Smalley, I. J. (1994) Particle packing from an earth science point of view. *Earth Science Reviews*, **36**, 59–82.

Rothfuchs, G. (1935) Particle size distribution of concrete aggregates to obtain greatest density. *Zement*, **24**(1), 5–12.

Rowe, P. W. (1962) The stress dilatancy relation for static equilibrium of an assembly of particles in contact. *Proceeding Royal Society*, **269A**, 500–527.

Rowe, P. W. (1969) The relation between the shear strength of sands in triaxial compression, plane strain and direct shear. *Géotechnique,* **19**(1), 75–86.

Shibuya, S., Mitachi, T. and Tamate, S. (1997) Interpretation of direct shear box testing of sands as quasi-simple shear. *Géotechnique*, **47**(4), 769–790.

Smalley I. J. and Dijkstra, T. A. (1991) The teton dam (Idaho, USA) failure; problems with the use of loess material in earth-dam structures. *Engineering Geology*, **31**, 197–203.

Tavenas, F. and La Rochelle, P. (1972) Accuracy of relative density measurements. *Géotechnique*, **22**(4), 549–562.

Taylor, D. W. (1948) *Fundamentals of Soil Mechanics*. Wiley, New York.

Thevanayagam, S. and Mohan S. (2000) Intergranular state variables and stress-strain behaviour of silty sands. *Geotechnique*, **50**(1), 1–23.

Vallejo, L. E. and Mawby R. (2000) Porosity influence on the shear strength of granular material–clay mixtures. *Engineering Geology*, **58**, 125–136.